OFFICE OF climate change
Queensland Climate Change Centre of Excellence
Research Report

Department of Environment and Resource Management

Rainfall in Queensland

Part 4: The ability of HiGEM to simulate Queensland's rainfall variability and its drivers

Prepared by Nicholas Klingaman

February 2012

Walker INSTITUTE

National Centre for Atmospheric Science
NATURAL ENVIRONMENT RESEARCH COUNCIL

Toward Tomorrow's Queensland

Queensland Government

Prepared by:

Nicholas P. Klingaman, Walker Institute for Queensland Climate Change Centre of Excellence,

Department of Environment and Resource Management

GPO Box 2454

Brisbane Qld 4001

ISBN 978-0-9805641-1-2

Disclaimer

This document has been prepared with all due diligence and care, based on the best available information at the time of publication. The department holds no responsibility for any errors or omissions within this document. Any decisions made by other parties based on this document are solely the responsibility of those parties. Information contained in this document is from a number of sources and, as such, does not necessarily represent government or departmental policy.

If you need to access this document in a language other than English, please call the Translating and Interpreting Service (TIS National) on 131 450 and ask them to telephone Library Services on +61 7 3224 8412.

This publication can be made available in an alternative format (e.g. large print or audiotape) on request for people with vision impairment; phone +61 7 3224 8412 or email <library@derm.qld.gov.au>.

Citation:

Klingaman, N.P., 2012: The ability of HiGEM to simulate Queensland's rainfall variability and its drivers. QCCCE Research Report: Rainfall in Queensland. Part. 4. Department of Environment and Resource Management, Queensland Government, Brisbane, Australia. Available online at www.derm.qld.gov.au.

To contact the author:
E-mail: n.p.klingaman@reading.ac.uk
Post: Department of Meteorology
University of Reading
Earley Gate, P.O. Box 243
Reading, Berkshire RG6 6BB
United Kingdom

Acknowledgements

Dr Nicholas Klingaman was funded by a grant from the Queensland Government, under a collaboration between the Queensland Climate Change Centre of Excellence (QCCCE) and the Walker Institute for Climate System Research at the University of Reading (http://www.walker-institute.ac.uk). Dr Klingaman was supervised by Steve Woolnough of the Walker Institute and Jozef Syktus of QCCCE. Dr Klingaman acknowledges productive discussions with Ken Day of QCCCE.

SILO rainfall data were provided by the Queensland Government. 20th Century Reanalysis V2 data were provided by the NOAA/OAR/ESRL PSD, Boulder, Colorado, USA, from their Web site at http://www.esrl.noaa.gov/psd/. Support for the Twentieth Century Reanalysis Project dataset is provided by the U.S. Department of Energy, Office of Science Innovative and Novel Computational Impact on Theory and Experiment (DOE INCITE) program, and Office of Biological and Environmental Research (BER), and by the National Oceanic and Atmospheric Administration Climate Program Office. HadISST SSTs were provided by the British Atmospheric Data Centre, under agreement with the U.K. Met Office. IBTrACS data were provided by the U.S. National Climatic Data Centre. HiGEM model output data were provided by the National Centre for Atmospheric Science in the United Kingdom.

Published February 2012

Contents

List of figures

List of tables

1 Executive Summary

Stakeholders and policymakers are seeking detailed information on the impacts of climate change and variability, especially on rainfall, at the local and regional levels. This information can be delivered by only those global climate models that represent the atmosphere and ocean at fine resolution, to robustly simulate the weather systems that produce rainfall. These models provide us with a better understanding of the key meteorological phenomena that affect Queensland. That knowledge can then be used to improve the simulation of these phenomena in lower-resolution climate models. Implementing these improvements will provide more accurate predictions on weekly to seasonal and decadal timescales, as well as more robust predictions of the impacts of climate change on these phenomena.

High-resolution Global Environment Model, version 1.1 (HiGEM) is a global, coupled climate model that was developed by the U.K. academic community. It is based on the U.K. Hadley Centre's HadGEM1 model, but HiGEM has considerably higher resolution: 90 km in the atmosphere and 30 km in the ocean. HiGEM has been used in this research as its increased resolution may allow the model to better represent regional climate variability and change in Queensland.

In this research, a 150 year control simulation of HiGEM was assessed to evalute the ability of the model to simulate Queensland's rainfall and its inter-annual and decadal variability. HiGEM was also assessed for its ability to produce the observed Empirical Orthogonal Teleconnection (EOT) patterns of rainfall avariability obtained from the SILO gridded rainfall dataset.

In the mean, HiGEM produces less rainfall over Queensland than observed, particularly in the north of the state. Most of this dry bias occurs because the model simulates a weaker Australian summer monsoon than is observed. However, HiGEM represents well the relationship between the El Niño Southern Oscillation (ENSO) and Queensland rainfall, on annual and seasonal timescales. The model even captured the observed asymmetric correlation between the ENSO and Queensland rainfall: stronger La Niña events cause stronger flood years in Queensland, but stronger El Niño events do not cause stronger droughts.

The research found that HiGEM lacks the ability to model decadal variations in Queensland rainfall and in the teleconnection between the ENSO and rainfall. This is likely due to the model's inability to simulate the Interdecadal Pacific Oscillation (IPO), which has been identified as the key driver of these variations.

In relation to the generation of tropical cyclones, HiGEM captures the observed regions of tropical-cyclone formation and the correct distributions of tropical cyclone tracks, but simulates too many tropical cyclones in the Southwest Pacific.

When EOT analysis is applied to HiGEM and the results are compared with the EOT patterns computed using observed rainfall, HiGEM performs well for those EOTs related to the ENSO in summer, winter and spring. HiGEM also represents the relationship between Southeast Queensland rainfall and onshore easterly winds, including the decadal variations in the winds' strength and moisture content. Futher, HiGEM correctly simulates the observed association between the frequency of tropical cyclones and summer rainfall in Cape York.

The success of HiGEM at reproducing many of the observed EOTs, particularly in summer, increases our confidence in the model's ability to predict the impact of climate change on Queensland's rainfall and its drivers.

2 Introduction and objectives

There is considerable uncertainty in projections of rainfall changes in Australia in a warmer world. Suppiah et al. (2007) demonstrated that the coupled climate models that contributed to the Intergovernmental Panel on Climate Change (IPCC) Fourth Assessment Report (AR4) produced a wide range of projected rainfall changes, extending from a 20 per cent increase per degree Celsius of global-mean warming to a 20 per cent decrease per degree Celsius. As global temperatures may increase by 2 degrees Celsius over the next fifty years, this uncertainty is considerable and limits the ability of society to successfully adapt to climate change. The uncertainty concerning how climate change will affect modes of inter-annual and decadal climate variability, such as the El Niño–Southern Oscillation (ENSO), is still greater.

As these modes of variability influence the frequency and intensity of rain-bearing weather systems such as tropical cyclones (e.g. Walsh and Syktus 2003) and east-coast cyclones (e.g. Hopkins and Holland 1997), the impacts of climate change on the spatial and temporal characteristics of rainfall may be considerably more uncertain than the change in the mean. Further, many of the climate models used for AR4 had horizontal grids too coarse to resolve these rain-bearing systems well, highlighting the need for finer-resolution coupled models. Suppiah et al. (2007) found that many models also displayed considerable biases in Australian temperature and rainfall in their "control" simulations with pre-industrial levels of carbon dioxide, although it is unclear whether such biases should necessarily hamper a model's ability to accurately simulate the response of the Australian climate to increased levels of carbon dioxide.

The Fifth Coupled Model Intercomparison Project (CMIP5) includes not only centennial climate-change simulations, but also a series of initialized decadal hindcasts and predictions (Taylor et al. 2009). The hindcasts will assess coupled models' ability to simulate the evolution of the climate system since 1960, while the predictions aim to improve understanding of the impacts of climate change over the next 10–30 years. The U.K. High-resolution Global Environment Model (HiGEM) is contributing to this decadal prediction experiment, using horizontal resolutions in the atmosphere and ocean much finer than the coupled models used for AR4 (Section 2.1). Such resolutions raise the prospect of more accurate simulations of regional-scale climate variability and change. Previous analysis of HiGEM has shown, for example, that its fine resolution improves the simulation of the ENSO, which is a key driver of Queensland's rainfall. The HiGEM CMIP5 decadal integrations therefore hold considerable promise for increased understanding of the predictability of Queensland's rainfall on timescales of 1–10 years.

Before undertaking analysis of the HiGEM CMIP5 decadal hindcasts and predictions, however, it is necessary to conduct a thorough evaluation of the model's ability to simulate Queensland's rainfall, its inter-annual and decadal variability and its relationship with known synoptic and climate drivers, such as the ENSO. This report builds upon the knowledge gained and techniques applied in Klingaman (2012a)—a summary of previous research into drivers of Queensland's rainfall—and Klingaman (2012b)—a detailed analysis of the drivers of state-wide and regional variations in seasonal rainfall in Queensland, as well as how the strengths of those drivers have changed over time.

In this report, the 150 year HiGEM control simulation is analysed in terms of Queensland's rainfall and its drivers. Section 2 describes HiGEM, the data to which the model is compared, and the method of empirical orthogonal teleconnection (EOT) analysis used to decompose the seasonal Queensland rainfall from HiGEM into patterns of coherent variability. Section 3 discusses the climatology and inter-annual and decadal variability of seasonal- and annual-mean Australian rainfall in HiGEM. The ability of HiGEM to simulate key drivers of Queensland rainfall, including ENSO and the Interdecadal Pacific Oscillation (IPO), is assessed in Section 4. The EOTs of seasonal HiGEM rainfall are compared to those computed from the SILO gridded analyses (Klingaman 2012b) in Section 5, to reveal which physical mechanisms underlying Queensland rainfall are robustly simulated in HiGEM and which are not.

3 Data and methods

3.1 HiGEM control simulation

This report analyses the output from a 150 year pre-industrial control simulation of the U.K. High-resolution Global Environment Model, version 1.1 (HiGEM) coupled atmosphere–ocean general circulation model (Shaffrey and others, 2009). HiGEM is a finer-resolution version of the Hadley Centre Global Environmental Model (HadGEM1; Ringer et al. 2006). In HadGEM1, the atmospheric and oceanic horizontal resolutions are 1.875° longitude × 1.25° latitude and 1° longitude × 1° latitude (refining to 0.33° latitude near the equator), respectively; in HiGEM these are 1.25° longitude × 0.83° latitude and 0.33° longitude × 0.33°, respectively. Both models have 38 (40) vertical grid points in the atmosphere (ocean). Numerous changes to the HadGEM1 physical parameterizations were made in HiGEM, which will not be discussed here; Shaffrey and others (2009) contains details of these.

For the atmosphere and land surface, the HiGEM control simulation was initialized from a European Centre for Medium-range Weather Forecasts (ECMWF) analysis. Ocean potential temperatures and salinities were set to September values from the World Ocean Atlas (Conkright et al. 2002); ocean currents were initialized at rest. The first several decades of the coupled control integration are therefore likely to be affected by the adjustment of the HiGEM ocean towards an equilibrium state. As in Shaffrey and others (2009), we discard the first 20 years of the integration and base our analysis on years 21–150 only.

Shaffrey and others (2009) and Roberts and others (2009) demonstrated that the finer atmospheric and oceanic resolutions in HiGEM considerably improved many aspects of the mean climate and inter-annual variability over HadGEM1. Most importantly for Queensland, relative to HadGEM1, HiGEM has a reduced dry bias over northern Queensland (Shaffrey et al. 2009, Fig. 6), a reduced easterly 850 hPa wind bias (Shaffrey et al. 2009, Fig. 10) and a more realistic spatial and temporal pattern of sea-surface temperature (SST) variability associated with the ENSO (Shaffrey et al. 2009, Figs. 19 and 20). The latter is linked to an improved simulation of the Pacific mean state in both SSTs and atmospheric circulation, which Roberts and others (2009) demonstrated was due in large part to HiGEM's ability to resolve tropical instability waves.

3.2 SILO gridded rainfall analyses

Means and inter-annual and decadal variability of seasonal and annual rainfall across Queensland were taken from the SILO dataset of kriged gauge values (Jeffrey 2001) on a 25 kilometre grid for the period March 1900–February 2008. Before comparing against HiGEM, the SILO data were linearly interpolated onto the HiGEM horizontal grid (Section 2.1) using an area-weighted method. Jeffrey (2001) used cross-validation to show that the monthly SILO totals were reliable across most of Queensland, with particular skill in coastal regions with high station densities, but were less skilful in the far north of the Cape York Peninsula where there are few stations with long records.

3.3 TRMM gridded rainfall analyses

As SILO covers only land points, seasonal and annual climatological precipitation from the Tropical Rainfall Measuring Mission (TRMM; product 3B42, version 6A) is used to evaluate climatological rainfall in HiGEM over the oceans surrounding Australia. TRMM data were available for 1999–2010 on a 25 kilometre grid. This record is substantially shorter than either SILO or the HiGEM control integration, but alternative products with longer records (e.g. from the Centre for Merged Analysis of Precipitation (CMAP)) either provide much coarser spatial resolution (e.g. 2.5° for CMAP) or do not provide continuous global coverage. TRMM is used only to determine biases in the HiGEM climatology over the oceans around Australia; all analysis of inter-annual and decadal variability uses SILO rainfall only. Once SILO and TRMM were interpolated to the HiGEM horizontal grid, the products were combined using the HiGEM land–sea mask: SILO at points that HiGEM considers land or fractionally land (i.e. "coastal tiled" points, see Shaffrey et al. (2009)); TRMM at points that HiGEM considers ocean.

3.4 HadISST sea-surface temperatures

Monthly-mean, 1900–2007 SSTs from the 1° × 1° Hadley Centre Sea Ice and SST dataset (HadISST; Rayner et al. 2003) are used to compute observed decadal variability in Pacific SSTs, for comparison with HiGEM. The observed Inter-decadal Pacific Oscillation (IPO) is calculated by the method of Folland et al. (1999) and Arblaster et al. (2002), which uses empirical orthogonal functions (EOFs) of 13 year lowpass-filtered seasonal-mean SSTs between 40°S–60°N.

3.5 HadCM3 control simulation

Pacific decadal variability in HadISST and HiGEM is compared to that from the 1000 year control integration of the Hadley Centre coupled model, version 3 (HadCM3; Gordon et al. 2000). The IPO in HiGEM is identified using the EOF technique described in section 2.4 above. For consistency with the 150 year HiGEM control integration, both the total decadal SST variability and the IPO are computed from consecutive 150 year periods in HadCM3, beginning with year 101 (e.g. years 101–250, years 251–400). Decadal variability in HiGEM, HadCM3 and HadISST is analysed in Section 4.2.

3.6 Tropical cyclone tracks

Observed tropical cyclone tracks for the South Pacific basin were obtained from the International Best Track Archive for Climate Stewardship (IBTrACS; Knapp et al. 2010) for October–May seasons during 1950–2008. Although observational coverage of the basin was limited prior to the satellite era, this longer period is chosen for better correspondence with the 130 years of the HiGEM control integration. To generate statistics of tropical-cyclone activity such as track, genesis and lysis densities on a regular grid, the IBTrACS tracks were processed by the method of Hodges (1996). Cyclone densities are expressed in units of storms per season within a 5° radius spherical cap of each T62 (approximately 1.9° longitude × 1.9° latitude) grid point; the unit area is approximately equal to 10^6 kilometre squared.

Tropical cyclone tracks from HiGEM were detected by the method of Thorncroft and Hodges (2001), in which tropical and extra-tropical cyclones are separated by their vertical structure: cyclones must display a warm-core structure and must attain a near-surface 20 meters per second wind speed before being classified as "tropical". Cyclone statistics from HiGEM were obtained from tracks in precisely the same manner as for IBTrACS, using October–May as the tropical-cyclone season in the South Pacific. It is important to note that cyclones in HiGEM continue to be tracked after they become extra-tropical, while the extra-tropical parts of the cyclone track are not included in the IBTrACS statistics. This leads to considerably longer tracks in HiGEM, as well as variations in cyclone lysis locations; the impacts of this will be discussed in Section 4.3.

3.7 Empirical orthogonal teleconnection analysis

Empirical orthogonal teleconnection (EOT) analysis is used to determine whether HiGEM is able to represent the influences of observed atmospheric drivers on inter-annual and decadal Queensland rainfall variability. EOT analysis was performed on seasonal-mean Queensland rainfall, using an identical procedure to that employed by Klingaman (2012b) on the SILO dataset for Queensland and by Smith (2004) on rainfall across Australia. The first six EOTs from HiGEM were computed for each three-month season: December–February (DJF), March–May (MAM), June–August (JJA) and September–November (SON). While Klingaman (2012b) analysed only the first three EOTs from SILO, the first six EOTs were computed for HiGEM to increase the probability of finding a HiGEM EOT that closely matched one of the three leading SILO EOTs. None of the fifth or sixth HiGEM EOTs matched any of the first three SILO EOTs, however, so only the four leading HiGEM EOTs are considered further.

The four leading HiGEM seasonal EOTs, the fraction of the variance in the HiGEM area-averaged Queensland rainfall that each explains, and correlations with various indices of atmospheric drivers are given in Table 1, which is printed near the discussion of the EOTs and their drivers (Section 5) for ease of reference. This table is similar to Table 1 from Klingaman (2012b)—reproduced in Appendix A (Table 3)—with one notable difference: the HiGEM table contains no correlations between the EOTs and the Inter-decadal Pacific Oscillation (IPO). The reasons for this are given in Section 4.2.

To identify the atmospheric driver of each HiGEM EOT and make comparisons with the observed drivers from Klingaman (2012b), regressions of each HiGEM EOT onto HiGEM seasonal-mean mean sea-level pressure (MSLP), 850 hPa zonal and meridional wind (u850 and v850), 500 hPa zonal and meridional wind and specific humidity (u500 ,v500 and q500) and SST are performed. Regressions of each EOT onto the seasonal standard deviations in HiGEM 2–10 day bandpass-filtered MSLP (MSLP2–10d) are used to identify anomalies in synoptic activity. While regressions of all four EOTs against all fields were performed, only those regressions relevant to each identified driver will be shown.

4 Queensland rainfall in HiGEM and its inter-annual and decadal variability

HiGEM shows consistent mean-state dry biases over northern and eastern Queensland, with wet biases just offshore (Fig. 1c). The biases are roughly proportional to the seasonal-mean rainfall, with DJF (Fig. 1f) and MAM (Fig. 1i) displaying much greater errors than JJA (Fig. 1l) and SON (Fig. 1o). These biases are not due to the use of different climatologies for land (SILO) and ocean (TRMM) grid points, as the SILO and TRMM annual-mean (Fig. 2) and seasonal-mean (not shown) climatologies are remarkably similar over Australian land points, except that SILO is slightly drier than TRMM across northern Queensland. Rather, HiGEM generates too much precipitation over the ocean, draining moisture out of the air before it reaches land and leading to dry biases. This pattern of biases may be due to the "coastal tiling" scheme in HiGEM, in which small fractions of near-coastal grid points that would ordinarily be entirely ocean are instead assigned the surface properties of land grid points. The scheme is designed to smooth the transition between land and ocean in the model, but it results in the atmospheric circulation responding to the coastline prior to the flow reaching the continent, which may lead to rising motion and precipitation over the ocean instead of over land.

To assess the inter-annual variability in rainfall in HiGEM, the normalized inter-annual standard deviations are computed for HiGEM and SILO: at each grid point, the HiGEM or SILO inter-annual standard deviation is divided by the HiGEM or SILO climatological rainfall. The ratios of these normalized standard deviations evaluate whether, for its own climatology, HiGEM has the same level of variance on inter-annual temporal scales as the SILO analyses. HiGEM performs relatively well for variability in annual means (Fig. 3a), with slightly higher-than-observed variability along the coast and lower-than-observed variability inland. The same spatial structure exists for inter-annual variability in DJF (Fig. 3b), MAM (Fig. 3c) and SON (Fig. 3e) seasonal means. In JJA, however, HiGEM shows considerably stronger variance than SILO across much of Queensland (Fig. 3d), although as JJA is a dry season for most of the state, small changes in the standard deviation can have a considerable effect on this statistic. For the analysis of teleconnections of seasonal Queensland rainfall to large-scale drivers (sections 4 and 5), it is promising that HiGEM shows approximately the observed levels of inter-annual rainfall variability for both seasonal and annual means. Displaying the correct levels of total inter-annual variability is necessary, but not sufficient, for producing rainfall responses of the correct magnitude to climate drivers on these temporal scales.

On decadal temporal scales, however, the variability in HiGEM rainfall displays considerably higher biases than for inter-annual scales (Fig. 4). Decadal variability is evaluated using the same ratio of normalized standard deviations as for inter-annual variability, but the time series of annual-and seasonal-mean rainfall were first smoothed using an 11 year running mean to emphasize the decadal component. HiGEM has far too little decadal variability in annual-mean rainfall across much of central Australia, including the western portions of Queensland (Fig. 4a), although the HiGEM normalised standard deviation is close to that for SILO in central and coastal Queensland. As for the inter-annual variability, the pattern of biases in DJF decadal variability (Fig. 4b) resembles that for annual mean, which is reasonable as much of Queensland rain falls in DJF., giving that season a higher weighting in annual mean. JJA rainfall in HiGEM again displays excessive variability in most of Queensland (Fig. 4d), including some regions where the annual mean was deficient, while MAM (Fig. 4c) and SON (Fig. 4e) are closer to SILO.

The results for the decadal temporal scales are less encouraging than those for the inter-annual ones, but HiGEM does produce adequate decadal variation in central and coastal Queensland. These near-observed levels of variability in HiGEM are not due to compensation errors between seasons, as all four seasons show realistic variability in these regions, except for JJA in south-eastern Queensland. Section 4.2 discusses a hypothesis for why decadal variability maybe lower than observations.

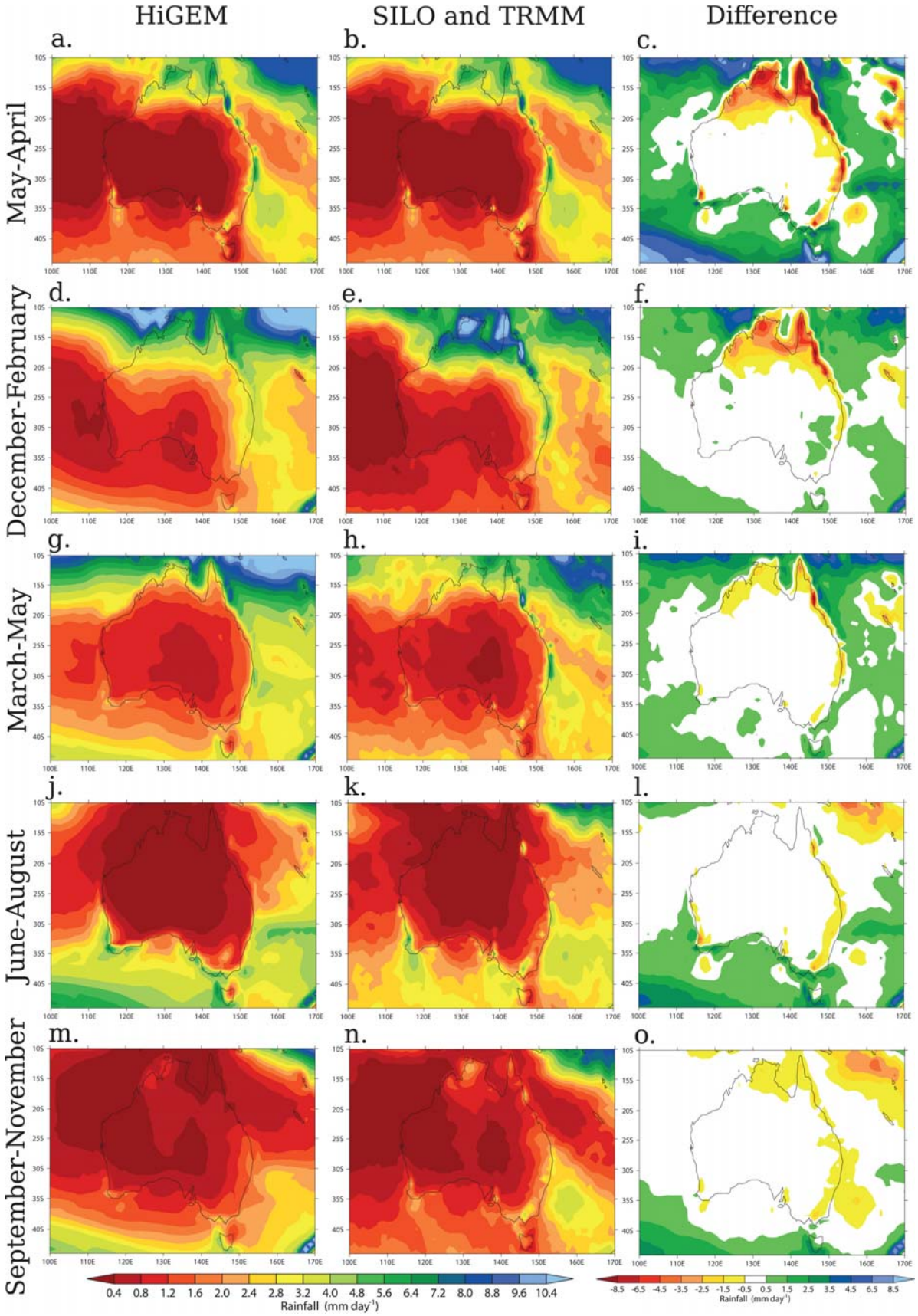

Figure 1: Climatological precipitation (mm day^{-1}) from (left) HiGEM and (centre) a combination of SILO (over land) and TRMM (over the ocean); (right) HiGEM minus the SILO/TRMM combination. The top row shows annual means; the lower four rows display seasonal means.

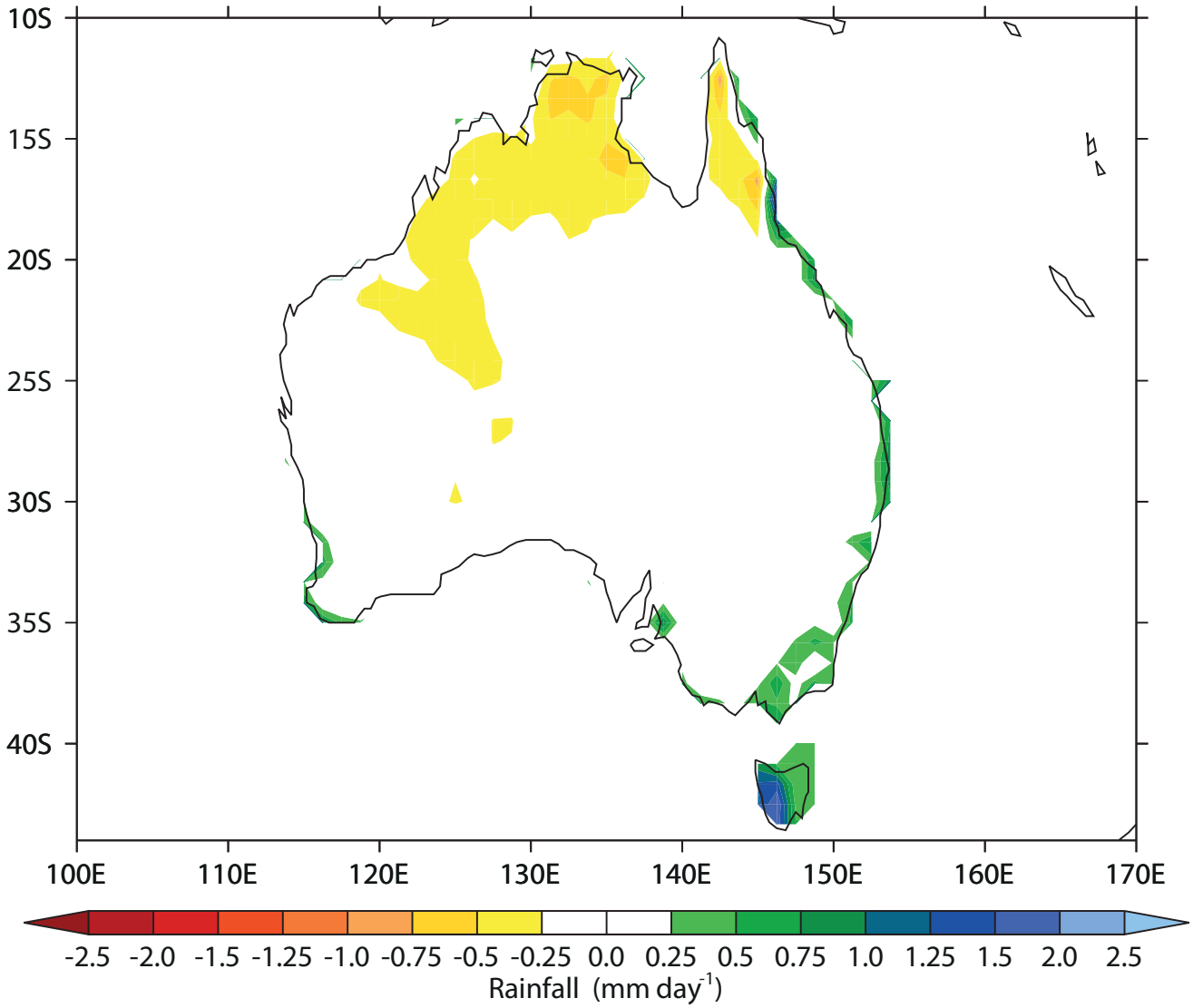

Figure 2: The difference in climatological and annual mean precipitation (mm day^{-1}) between SILO (1900-2008) and TRMM (1999-2010) over Australian land points, taken as SILO minus TRMM.

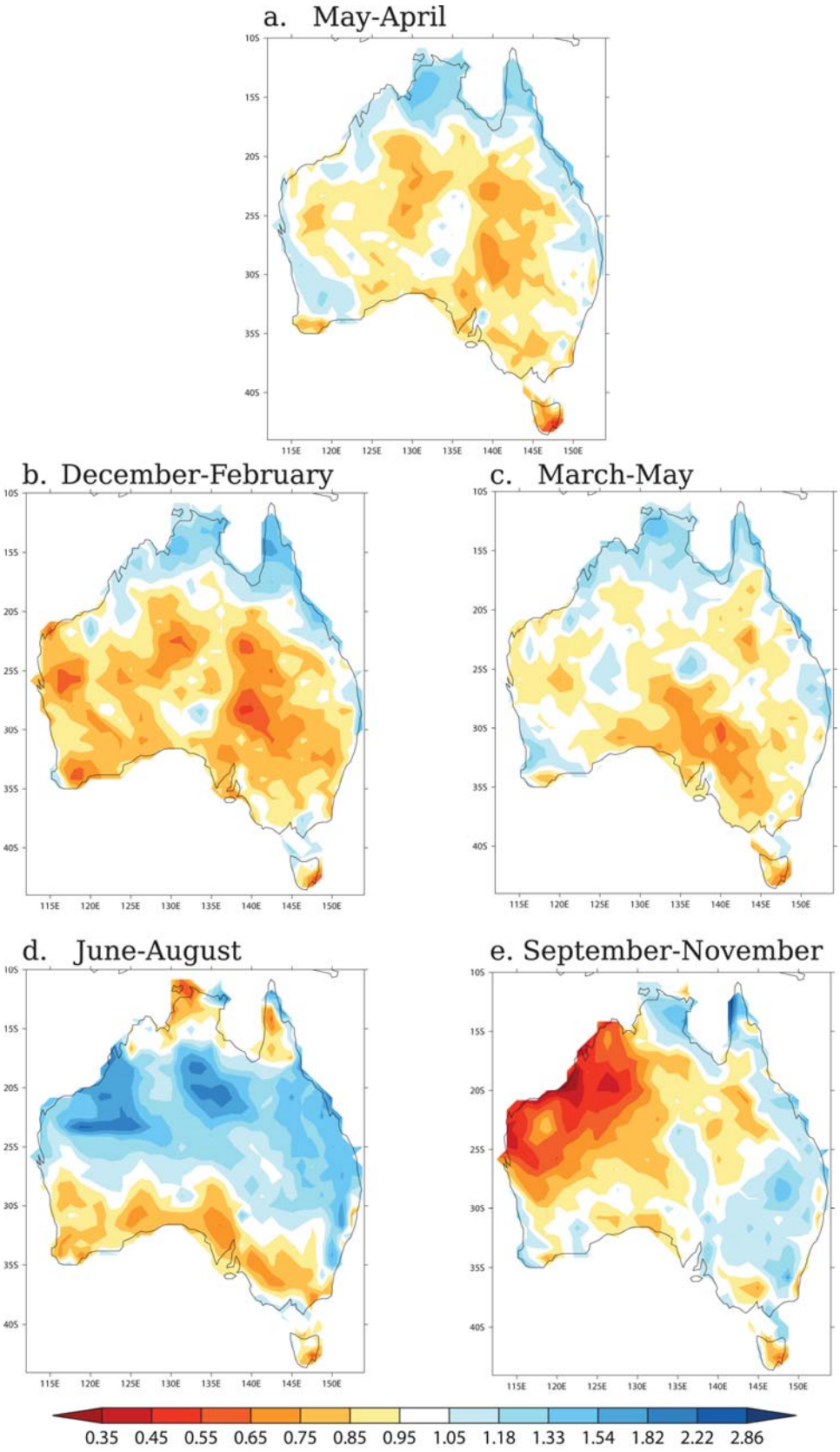

Figure 3: Ratios of normalised (by climatological precipitation) inter-annual standard deviation in precipitation (unit less) for HiGEM divided by SILO, using (a) annual-mean precipitation and (b-e) seasonal means for (b) DJF, (c) MAM, (d) JJA and (e) SON.

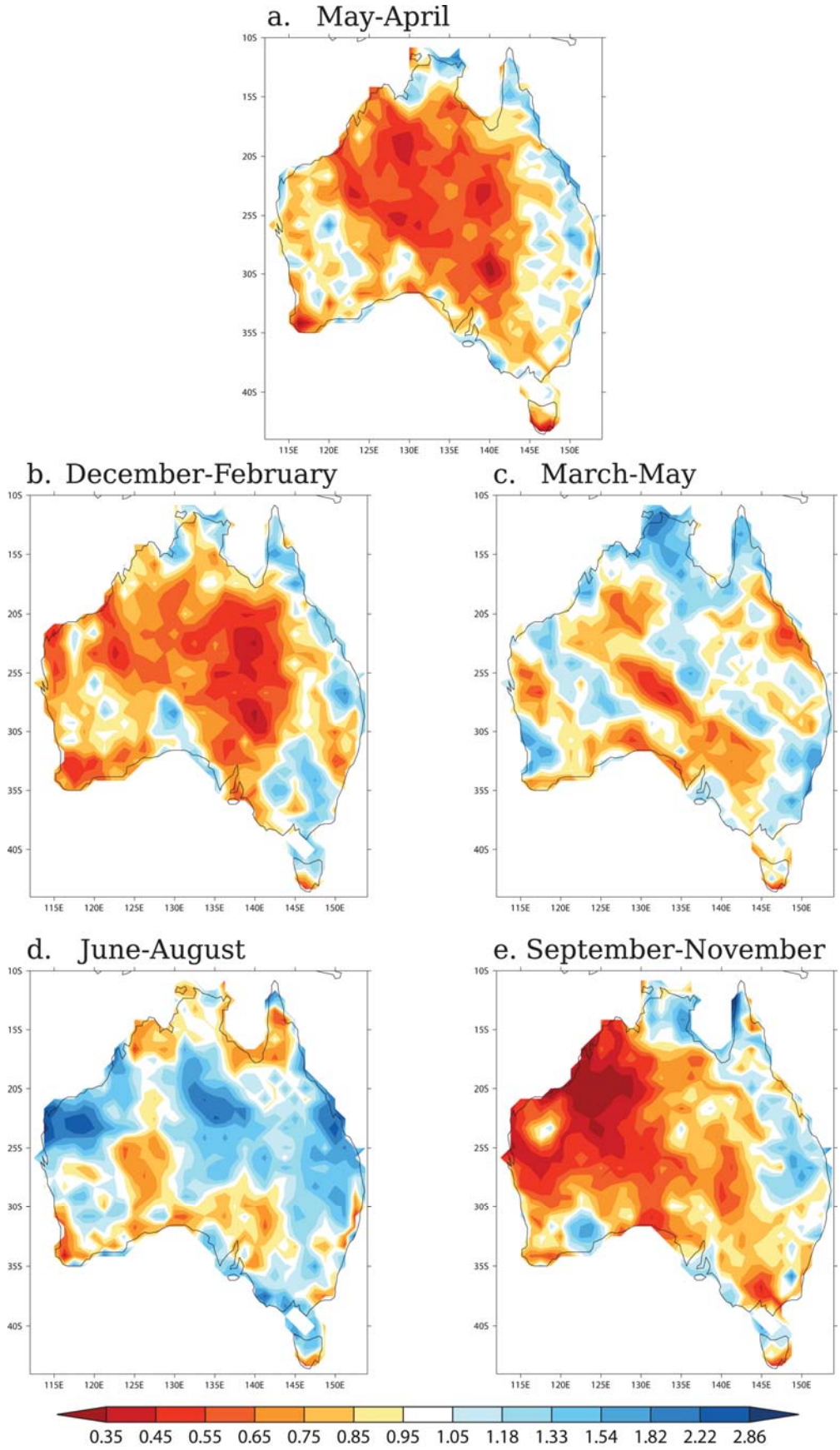

Figure 4: As in Figure 3, but using ratios of normalised inter-annual standard deviations in 11-year running-mean precipitation, to emphasize decadal variability.

5 The ability of HiGEM to simulate known drivers of Queensland rainfall variability

5.1 The El Nino–Southern Oscillation

Shaffrey et al. (2009) and Roberts et al. (2009) contain a detailed analysis of the spatial and temporal pattern of the ENSO in HiGEM, which will not be repeated here. Instead, this report focuses on the fidelity of the teleconnection in HiGEM between the ENSO and Queensland rainfall.

HiGEM successfully simulates a negative correlation of approximately the observed magnitude (from SILO and HadISST; Fig. 5a) between May–April annual-mean Niño 4 SST anomalies and May–April annual-mean rainfall across Queensland (Fig. 5b). Similar to observations (e.g., Murphy and Ribbe, 2004; Hendon et al., 2007), HiGEM produces a stronger correlation between Queensland rainfall and the central Pacific Niño 4 index than the eastern Pacific Niño 3 (not shown). The May–April annual mean is used to limit mixing phases of the ENSO in a single annual period, as the ENSO often changes sign during austral autumn. The HiGEM correlation is weaker than observed across northern Australia, which is likely due to low correlation magnitudes in HiGEM during MAM (Fig. 5h) relative to SILO/HadISST (Fig. 5d). Klingaman (2012b) found that the third MAM EOT of SILO rainfall, which described coherent rainfall variations in the Cape York Peninsula and across northern Australia, was associated with the impact of the ENSO on the strength of the late-season monsoon. The weak correlations in HiGEM in MAM may indicate that these ENSO–late-monsoon interactions are missing or suppressed in HiGEM; section 5 explores this further. In DJF (Figs. 5c and 5g), JJA (Figs. 5e and 5i) and SON (Figs. 5f and 5j), the strength and spatial pattern of the Niño 4–Queensland rainfall correlations in HiGEM closely resemble those in observations, although the HiGEM correlation is occasionally too strong. With the exception of the Cape York Peninsula, the ENSO in HiGEM explains a similar fraction of variance (approximately 30 per cent) in Queensland rainfall as the observed ENSO.

Lag correlations of area-averaged Queensland rainfall (land points in 138° –154°E, 9°–29°S) and Niño 4 SSTs reveal that while winter, spring and early summer HiGEM rainfall shows similar predictability from Niño 4 (Fig. 6b) as observations (Fig. 6a), late summer and autumn rains in HiGEM are only weakly predictable from the ENSO. In both HiGEM and SILO/HadISST, June Niño 4 SSTs are strongly correlated with rainfall from June through December, as demonstrated by the downward (i.e. longer lead time) slope of the correlation contours in June–December. In HiGEM, however, January rainfall displays an erroneously strong correlation with Niño 4 at long lead times, while the February–April lag correlations are much weaker than observed. The positive correlations in HiGEM for positive lags (i.e. rainfall leading Niño 4) in February and March are indicative of overly bi-annual ENSO variability; in other words, the ENSO in HiGEM too often switches sign in austral El Niño years. Further, the correlation for La Niña years is not affected by the outlying years, as when the four strongest La Niña events—those with May–April mean Niño 4 < -1.0°C—are removed, the correlation coefficient weakens only slightly (the dashed blue line in Fig. 7a).

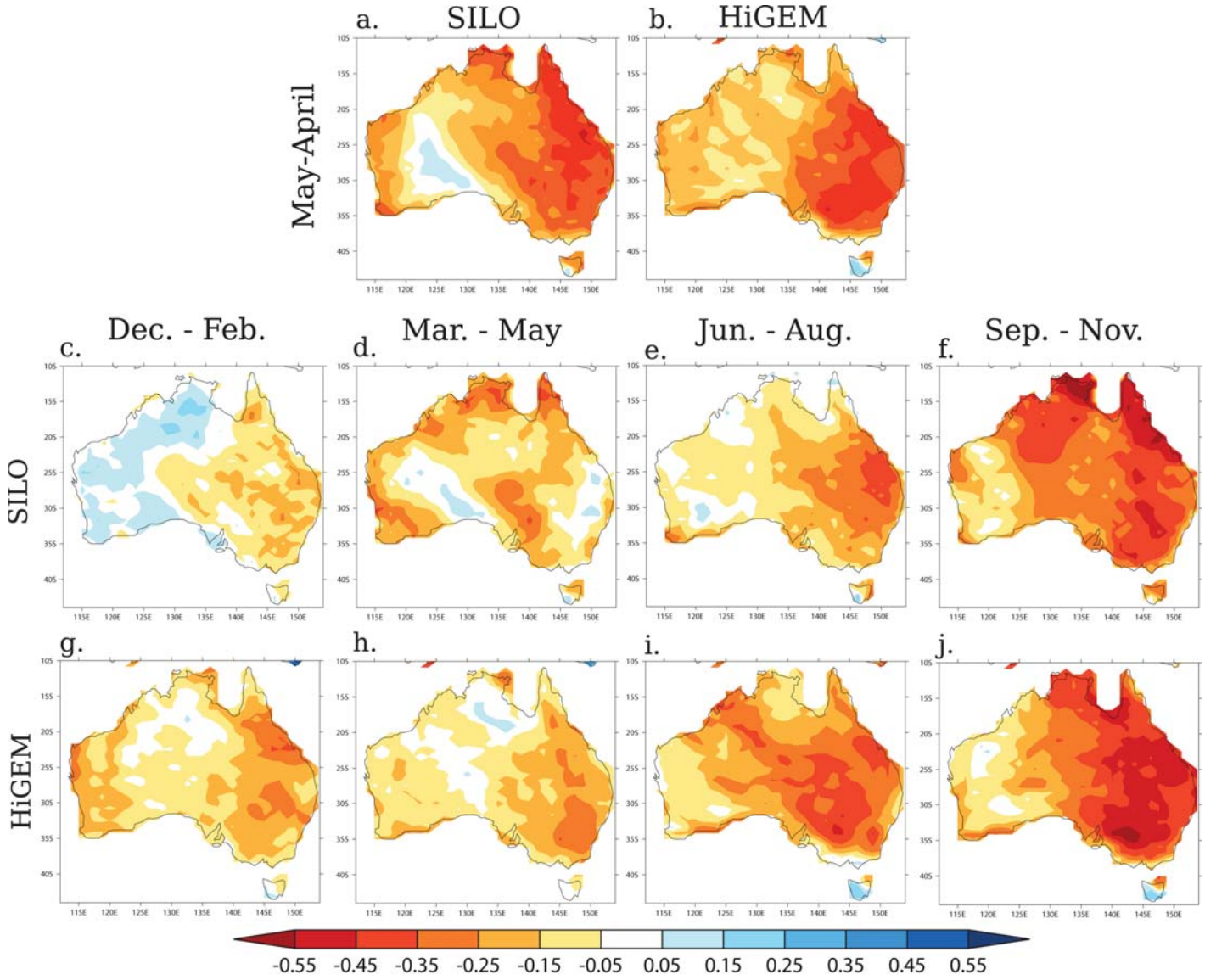

Figure 5: Instantaneous correlations between (a–b) May–April annual-mean (a) SILO rainfall and HadISST Niño 4 SSTs and (b) HiGEM rainfall and Niño 4 SSTs; (c–f) seasonal-mean SILO rainfall and HadISST Niño 4 SSTs for (c) DJF, (d) MAM (e) JJA, (f) SON; (g–j) as in (c–f) but for HiGEM rainfall and Niño 4 SSTs.

The HiGEM control integration successfully reproduces the observed asymmetric rainfall–Niño 4 relationship (Fig. 7b), with a highly significant correlation between Queensland rainfall and Niño 4 SSTs under La Niña but not under El Niño. The magnitudes of the correlations are remarkably similar to observations. The La Niña–rainfall relationship weakens somewhat when La Niña events with annual-mean SST anomalies < -1.0°C are removed (dashed blue line in Fig. 7b), more so than in observations, indicating that the agreement between HiGEM and observations is due in part to these outlying La Niña years in HiGEM. HiGEM produces quite a few strong La Niña events, three of which—those with cool anomalies stronger than -1.5°C—are stronger than any in the 1900–2008 HadISST record; the strongest two La Niñas are also the two wettest years in Queensland.

The ENSO–Queensland rainfall teleconnection is well-simulated in HiGEM, in terms of the instantaneous (Fig. 5) and lead–lag relationships (Fig. 6), the seasonal cycle of the correlation magnitude (Fig. 5) and the asymmetric response of rainfall to Niño 4 anomalies of opposite sign. There are still some minor deficiencies in HiGEM, though, including a weak rainfall–ENSO relationship in northern Queensland in autumn (Fig. 5f), an overly bi-annual ENSO period that affects the lead–lag relationships (Fig. 6b), and the fact that the La Niña– rainfall correlation is dominated by a few very strong La Niña events (Fig. 7b).

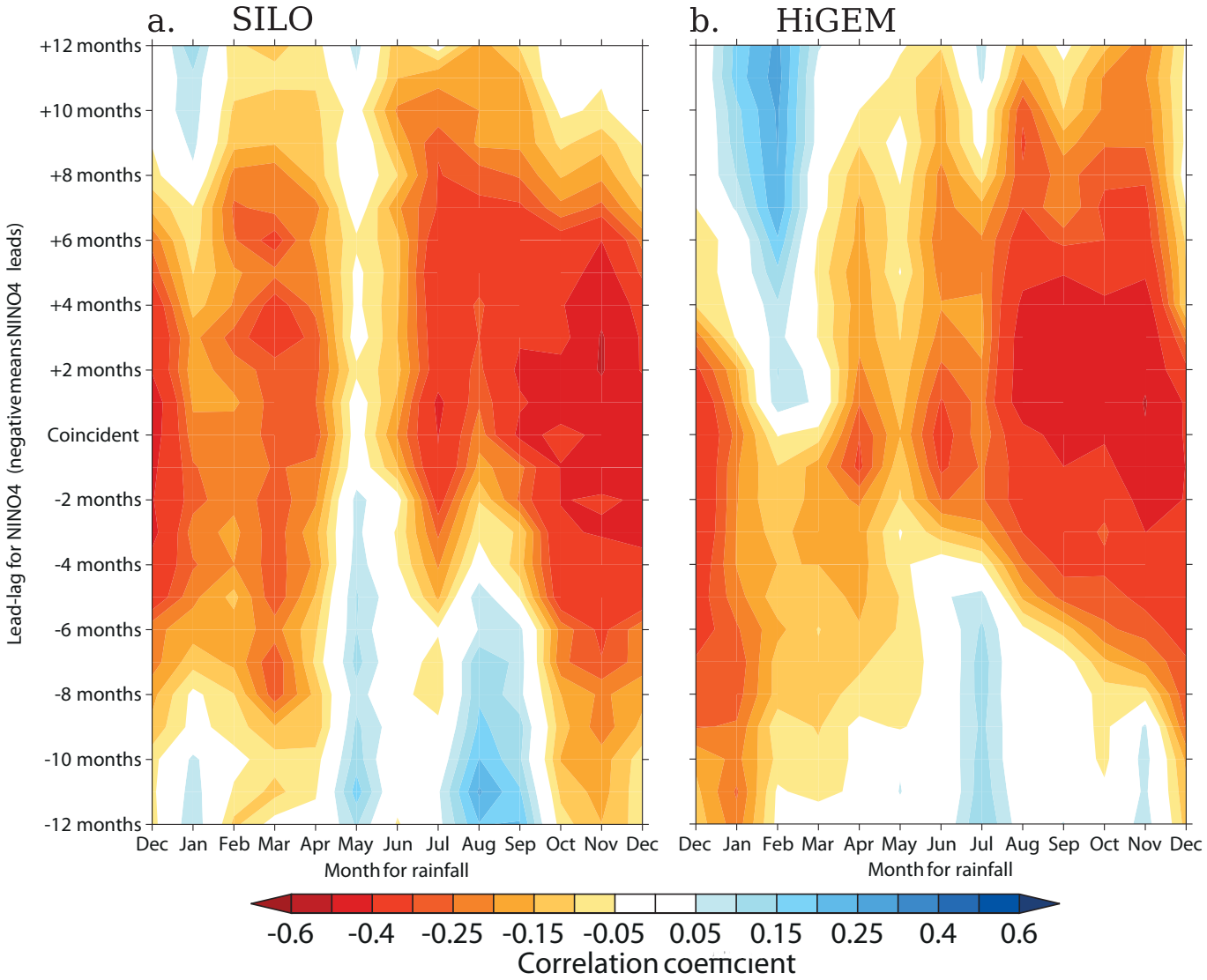

Figure 6: For (left) SILO rainfall and HadISST Niño 4 SSTs and (right) HiGEM rainfall and Niño 4 SSTs, lead–lag correlations between monthly-mean, area-averaged Queensland rainfall (138°–154°E, 9°–29°S) and monthly-mean Niño 4 SST anomalies. The horizontal axis gives the month for rainfall; the vertical axis gives the lead or lag time for Niño 4 SST anomalies, with negative (positive) values indicating that Niño 4 leads (lags) Queensland rainfall.

5.2 The Inter-decadal Pacific Oscillation

To detect the IPO in HadISST and the HiGEM and HadCM3 control integrations, the procedure of Arblaster et al. (2002) was used, itself a modified version of that of Folland et al. (1999): EOFs of 13-year lowpass filtered monthly-mean SSTs were computed for the 109 years of HadISST data, the 150 years of HiGEM output and years 101–250 of the 1000-year HadCM3 integration (Sections 2.4 and 2.5 contain further details on this method). The full 150 years of HiGEM data are used here, to give a longer record for detecting decadal variability; the first and last 13 years of each dataset are lost to the filter. The HiGEM EOFs were also computed with the first few decades removed to account for ocean spin-up, as discussed in the next paragraph.

As in Arblaster et al. (2002), the IPO is the second EOF in HadISST, as the first EOF is a uni-polar mode representing the global warming signal. The characteristic tropical–extra tropical tri-pole IPO pattern can be seen clearly in Fig. 8a. In HiGEM (Fig. 8b) and HadCM3 (Fig. 8c), EOF 1 has the highest pattern correlation with HadISST EOF 2 of any of the first ten model EOFs. While HadCM3 EOF 1 strongly resembles HadISST EOF 2, HiGEM EOF 1 shows much stronger positive loading to the east of Japan and in the North Atlantic, with reduced

magnitudes in the tropics and in the Southern Hemisphere extra-tropics. The HiGEM EOF 1 also has the wrong sign—positive instead of negative—along the west coast of North America. Thus HiGEM EOF 1 appears to be dominated by variability in the Northern Hemisphere western-boundary-current regions, rather than in the tropical and sub-tropical Pacific Ocean. This is not caused by ocean spin-up during the first few decades, as the HiGEM EOFs were re-computed with the first 20, 40 and 60 years removed: the unrealistically high variances in the western Pacific and North Atlantic remained, with little variance in the equatorial Pacific.

Using 13-year lowpass filtered SSTs, linear regressions of grid point SSTs against Niño 4 SSTs were computed for HadISST, HiGEM and HadCM3 (Figs. 8d–f). In HadISST and HadCM3, these regressions show that on decadal temporal scales, there is considerable covariation in equatorial and off-equatorial Pacific SSTs: Niño 4 SSTs are positively correlated with SSTs in the sub-tropical Pacific, the Indian Ocean and along the western coasts of North and South America, with weak negative correlations in the north-western and south-western Pacific. In HiGEM, however, Niño 4 SSTs are correlated only with themselves and some small regions in the South Pacific. This reinforces the lack of coupling between tropical and extra-tropical decadal SST variations in HiGEM, which defined the IPO in observations. Similar linear regressions of 13-year lowpass-filtered SSTs were also performed for the Niño 3, Niño 3.4 and equatorial Pacific-wide (averaged 5°S–5°Nand 150°E–90°W) regions, with similar results as for Niño 4.

Wavelet transforms of monthly-mean, unfiltered Niño 4 SSTs confirm that HiGEM lacks decadal variability in equatorial Pacific SSTs: HadISST (Fig. 8g) shows considerable decadal and multi-decadal variability in Niño 4 throughout much of the 1900–2008 period; HadCM3 (Fig.8i) has much more variability on 4–8 year periods, but does have some decadal variability; HiGEM (Fig.8h) has nearly no decadal variability that is not tied to strong inter-annual variations. The strong peak in the 3–4 year period band in HiGEM near year 110 is due to two strong La Niña events, the same two that were associated with the two wettest years in Queensland (section 4.1). Such strong variability on the 3–4 year timescale inevitably projects onto the longer, decadal temporal scale, leading to the statistically significant 10–15 year signal in HiGEM. Otherwise, there is practically no decadal variability in HiGEM Niño 4. As for the linear regressions, wavelet transforms of Niño 3, Niño 3.4 and equatorial Pacific-wide SSTs were computed, with similar results as for Niño 4. The EOFs, regressions and wavelet transforms were also performed for the other five consecutive 150 year periods of the HadCM3 control integration (i.e. years 251–400, 401–550 and so on); these periods also showed IPO-like variability that was similar to observations and much stronger than HiGEM.

Alongside limited decadal variability in rainfall (Fig. 4) over much of Australia, HiGEM lacks an IPO, as defined by coherent tropical–extra-tropical decadal variability in SSTs. On decadal temporal scales, space–time variance in SSTs is dominated by strong signals in the Northern Hemisphere boundary-current regions (Fig. 8b), with few significant correlations between equatorial and off-equatorial Pacific SSTs (Fig. 8e) and little variability in Pacific equatorial SSTs themselves (Fig. 8h).

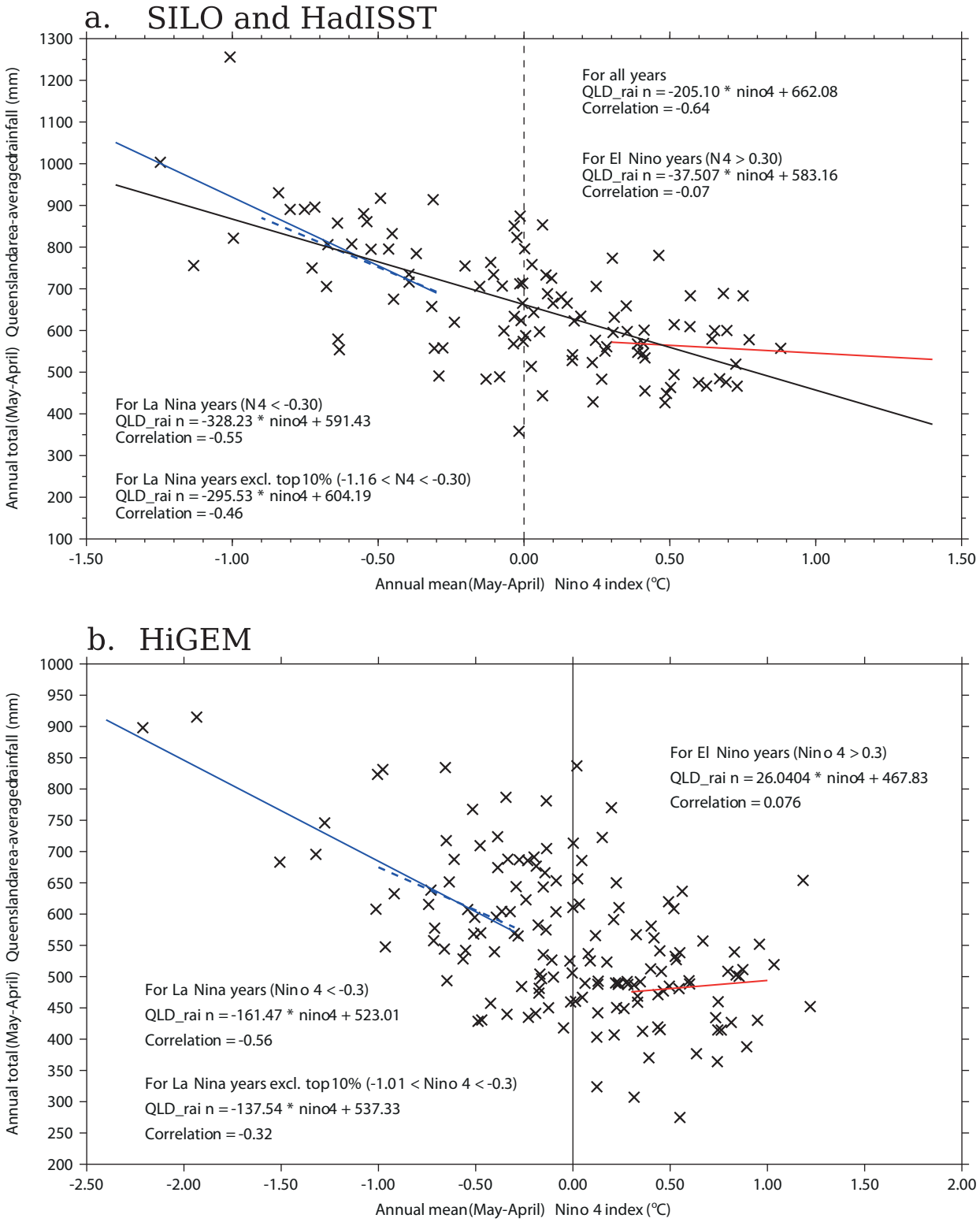

Figure 7: For (top) SILO rainfall and HadISST Niño 4 SSTs and (bottom) HiGEM rainfall and Niño 4 SSTs, scatter plots of the May–April annual mean Niño 4 SST anomalies against May–April annual-total, area-averaged (138°–154°E, 9°–29°S) Queensland rainfall. Linear-regression lines are shown for (black) all years, (solid blue) all years with a Niño 4 anomaly < -0.3°C (La Niña), (dashed line) all years with -1.0°C < Niño 4 anomaly <-0.3°C (weak or moderate La Niña), and (solid red) all years with a Niño 4 anomaly > 0.3°C.

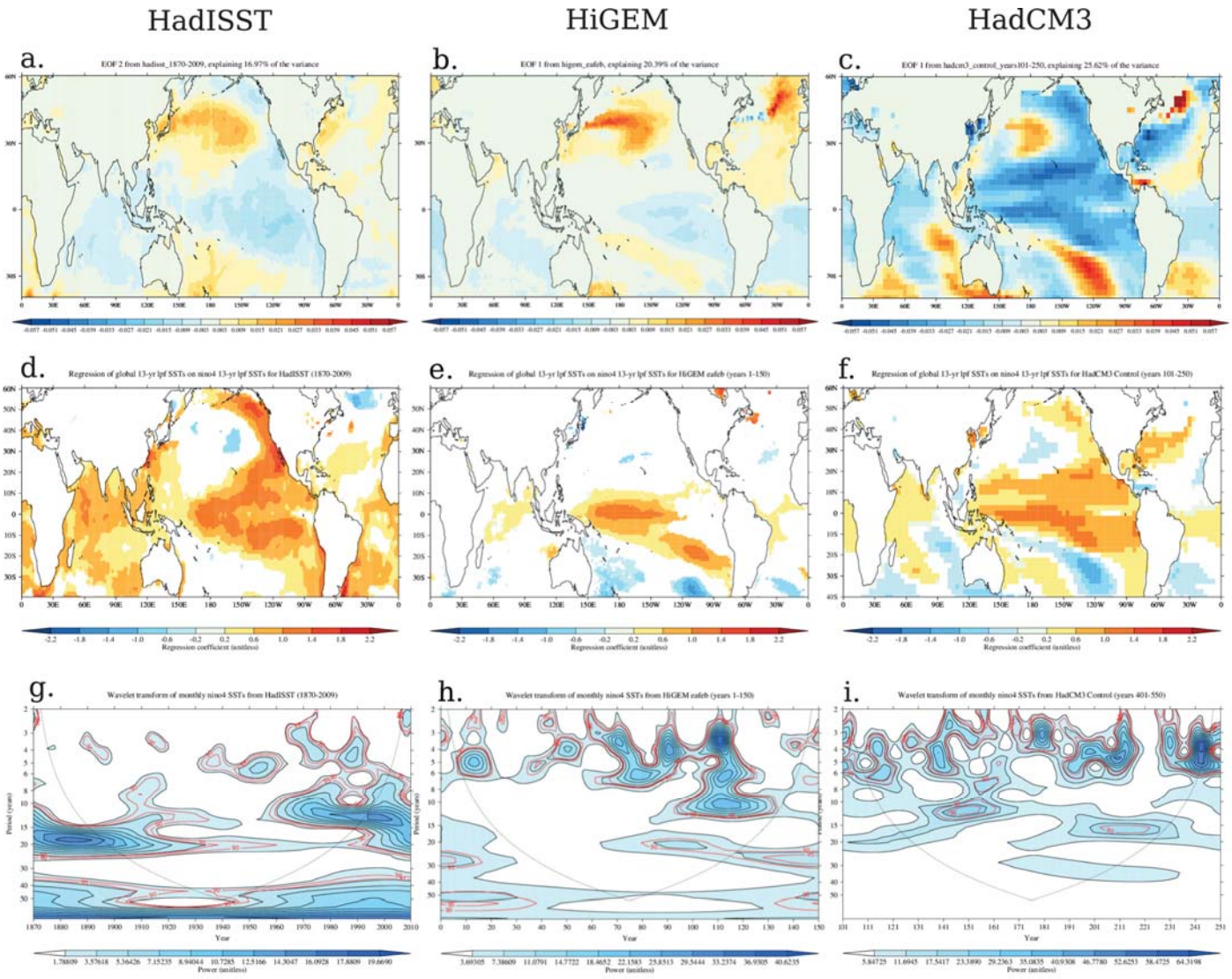

Figure 8: For (left) HadISST, (centre) the HiGEM control integration and (right) years 101–250 of the HadCM3 control integration: (top) the EOF of 13-year lowpass-filtered monthly-mean SSTs that most resembles the IPO; (middle) coefficients of linear regression of 13-year lowpass-filtered monthly-mean SSTs onto 13-year lowpass filtered monthly-mean Niño 4; (bottom) the wavelet transform of monthly-mean Niño 4 SSTs, using a Morlet mother wavelet, with the 90 per cent and 95 per cent confidence levels marked in red contours. Regression coefficients are shown only where correlations are statistically significant at the 5 per cent level. The dotted line in the wavelet diagrams shows the "cone of influence", outside of which edge effects dominate the signal and the results are not robust.

5.3 Tropical Cyclones

In its climatology, HiGEM produces more tropical cyclones tracks near the northern Australian coast (Fig. 9a) than observed (Fig. 9b), particularly west of the Gulf of Carpentaria. Near Queensland the HiGEM track densities resemble observations, although they are likely too many storms near the Cape York Peninsular and too few along the eastern coast further south (Fig. 9c). The long "tail" of HiGEM tracks extending southeast, past New Zealand, are due to continued tracking of cyclones after they become extra-tropical; these transitions are not included in observations (section 2.6). Still, HiGEM track densities are far too large east of the dateline.

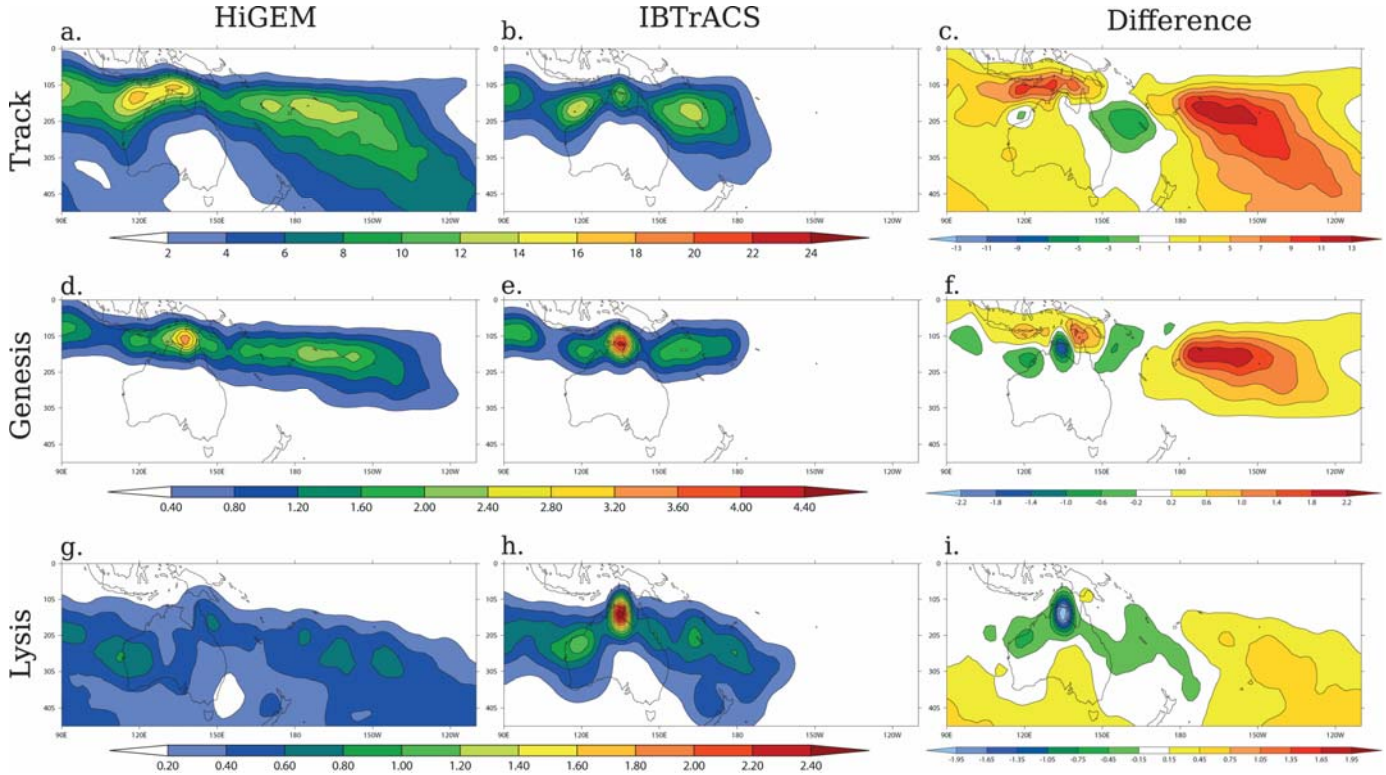

Figure 9: For (left) IBTrACS observations and (middle) HiGEM and (right) HiGEM minus IBTrACS: climatological October–May-mean (top) track density, (middle) genesis density and (bottom) lysis density of tropical cyclones. Densities are in units of cyclones season^{-1} within a 5° spherical cap of each T62 (approximately 1.9° × 1.9°) grid point. The unit area is approximately equal to 10^6 km^2; see section 2.6 for further details.

Most cyclones in HiGEM are generated just south of the Gulf of Carpentaria (Fig. 9d). The peak there is remarkably similar to the observed peak in genesis density (Fig. 9e). Genesis densities in the Coral Sea are also similar to IBTrACS (Fig. 9f), although, as seen in the track densities, HiGEM forms far too many tropical cyclones east of the dateline.

Many observed cyclones "die" near Darwin, with secondary maxima along the western and eastern coasts (Fig. 9h). HiGEM produces these secondary maxima well, but fails to simulate the maximum near Darwin (Fig. 9g). This is likely due to different treatment of extra-tropical transitions in IBTrACS and HiGEM; the fact that extra-tropical cyclones continue to be tracked in HiGEM leads to a wider variety of lysis locations that are generally further south than in observations (Fig. 9i).

While tropical cyclones are considered as potential drivers of rainfall EOTs in Section 5 - as they were in Klingaman (2012b) for observations - this report does not consider the inter-annual or decadal variability of tropical cyclones in HiGEM, or the connections in variability of those temporal scales to large-scale drivers (e.g. the ENSO).

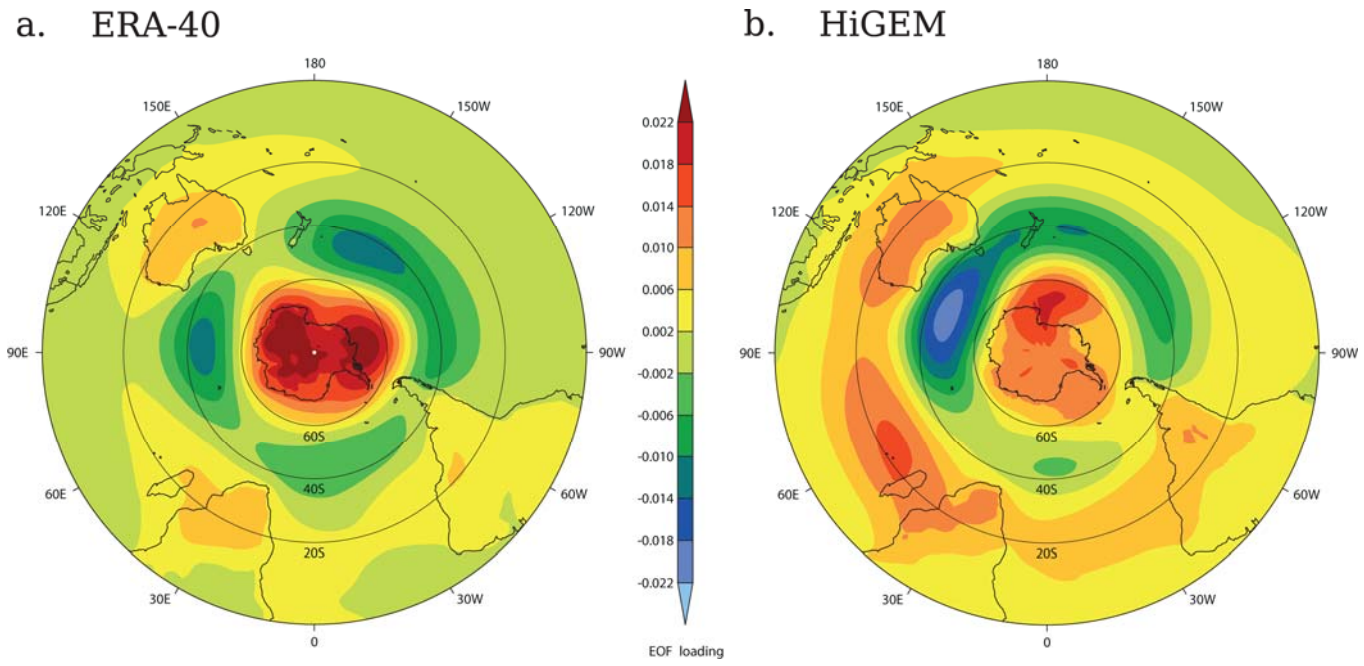

Figure 10: The spatial structure of the leading EOF of monthly-mean, Southern Hemisphere surface pressures in (left) ERA-40 and (right) HiGEM.

5.4 The Southern Annular Mode

The SAM frequently emerges as the first EOF of the southern hemispheric surface pressure in GCMs, observations and reanalysis data (e.g. Thompson and Wallace, 2000). Here, we compare the first EOFs of monthly-mean, Southern Hemispheric surface pressures in the 1958-2002 European Centre for Medium Range Weather Forecasting reanalysis (ERA-40; Uppala et al. 2005, Fig. 10a) and HiGEM (Fig. 10b). The HiGEM EOF broadly resembles that from ERA-40, but HiGEM has reduced variability over Antarctica - with the positive pole there shifted away from the South Pole - and increased variability in the Southern Ocean south of Australia. The SAM in HiGEM also has pronounced tri-pole pattern than in observations, with a stronger third, positive pole near 20°S. HiGEM EOF 1 explains 27.2 per cent of the total space-time variance in HiGEM Southern Hemisphere total pressure, similar to ERA-40 EOF 1, which explains 24.1 per cent of the ERA-40 variance.

The connection between HiGEM SAM and rainfall in Queensland is explained in Section 5, when the SAM is investigated as a potential driver for EOTs of HiGEM seasonal rainfall.